Complete Study of the Phase Advancing in the Switched Reluctance Motor/Standalone Generator

M. Asgar[1], E. Afjei[2], A. Siadatan[3]
1- Department of Electrical Engineering, Shahid Beheshti University G. C., Tehran, Iran
Email: m_asgar@sbu.ac.ir
2- Department of Electrical Engineering, Shahid Beheshti University G. C., Tehran, Iran
Email: e-afjei@sbu.ac.ir
3- Department of Electrical Engineering, West Tehran Branch, Islamic Azad University, Tehran, Iran
Email: a_siadatan@wtiau.ac.ir

Received: June 2012 Revised: Oct. 2012 Accepted: Dec. 2012

ABSTRACT:
The switched reluctance motor is a singly excited, doubly salient machine which can be used in the generation mode by selecting the proper firing angles of the phases. Due to its robustness, it has the potential and the ability to become one of the generators to be used in the harsh environment. This paper briefly discusses the energy conversion by a switched reluctance generator (SRG) when two switches per phase converter circuit and discrete position sensors are employed. It is well known fact that, as the generator's speed increases by a prime mover and the shape of the current waveform changes in such a way that limits the production of generating voltage. At high speeds, it is possible for the phase current never reaches the desired value to produce enough back-EMF for sufficient voltage generation, therefore, the output power falls off. In order to remedy this problem, the phase turn on angle is advanced in a way that the phase commutation begins sooner. Since one of the advantages of this type of generator is its variable speed then, the amount of advancing for the turn on angle should be accomplished automatically to obtain the desired output voltage according to the speed of the generator, meaning, as the generator speed increases so should the turn on angle and vice versa. In this respect, this paper introduces an electronic circuit in conjunction with time reshaping of the command pulses obtained from position sensors and the drive converter to achieve this task for a desired output voltage when a SRG feeding a resistive load. To evaluate the generator performance, two types of analysis, namely numerical technique and experimental studies have been utilized on a 6 by 4, 30 V, SRG. In the numerical analysis, due to the highly non-linear nature of the motor, a three dimensional finite element analysis is employed to calculate some of motor parameters and then using these parameter, current shape and magnitude are computed, whereas in the experimental study, a proto-type generator and its circuitries have been built and tested using two-switch per phase converter. A linear analysis of the current waveform for the generator under different advancements of the turn on angle has been performed numerically and experimentally and the results are presented.

KEYWORDS: SRG, SRM, Switched reluctance motor/Generator, Phase advancing.

1. INTRODUCTION

SRG can be considered as one of the attractive options for the worldwide increasing demand of the electrical energy. It is low cost, fault tolerant with a rugged structure and operates with acceptable efficiency over a wide speed range. Due to the lack of windings and permanent magnets on the rotor parts, the high rotational speeds and high-temperature are possible. Furthermore, the absence of windings on the rotor causes the majority of the losses to show up in the stator, making the SRG relatively easy to cool. There have been many researches on the SRG characteristics utilizing asymmetry half bridge converter [1]-[3]. The SRGs utilizing has been proved to be functional and useful for some applications such as the starter/generator of the gas turbine of the aircrafts [4], [5] the wind turbine generator [6]-[8] and the starter/alternator electric cars [9], [10]. The solid structure of SRG is useful for an ultra-high speed generator such as a micro gas turbine generator [11].

In [12], a new performance criterion as the productivity of the generator is described, in this method, instead of the two phase commutation steps, which are on and off in single pulse mode, a freewheeling step is added. During this step, the phase is short circuited and the current increases due to back-emf voltage. This method

produces more power than the conventional method, for the same turn on period.

The start and duration of the current pulses for each phase in a SRG are controlled and synchronized with rotor position by means of a direct or an indirect shaft positioning scheme. The performance of SRG can be greatly influenced by choosing the proper starting time for the phase turn on angle at different speeds [13]. The time duration τ available for the current in each phase winding is directly related to the speed of the generator. As the generator's speed increases the amount of time, τ, decreases and at some point, it can reach a certain value such that, the control of the winding current for obtaining a desired value of the output voltage/power is impossible even by setting the width of pulses at its maximum value (i.e. duty cycle = 1) in order to havethe highest attainable field current. At high speeds, the current cannot rise quickly enough in the phase winding to reach the preferred level. Due to this reason, it is desirable to get current into the generator phase winding before the phase inductance reaches the generating mode. Hence, turn on and turn off angles can be defined as control variables, where, turn on angle is set to accomplish the output power and the turn off angle is selected to achieve optimal efficiency at each power level and speed. . In general, there are two methods to boost the current rise time namely varying the dwell angle and the use of the smaller number of turns during the excitation mode can be considered. These options will allow keeping SRG output voltage constant at high speeds where current control (PWM) is not a possible option anymore.

2. EXCITATION AND GENERATION MODES OF OPERATION

In order to generate electrical energy by a SRGsome means of excitation are required. This excitation can be achieved by a converter circuit, one phase winding and its drive circuit shown in Fig. 1.

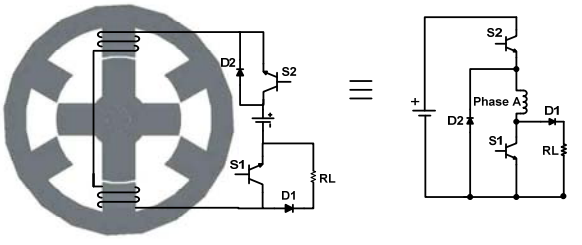

Fig. 1. A 6 by 4 SRG, one phase winding and its two switches per phase drive circuit

When the main switch, S1, is closed, the current builds in the SRG phase winding. Once the main switch is turned off, the more energy is returned to the source than that was provided for the excitation through the same winding. For the generator operation, the excitation generally begins near the aligned position for the relatively low-speed operation. The excitation is often advanced with increasing speed so that the excitation begins before the aligned position. This is analogous to the advance introduced in the control of the SRM [14]. At the start of the excitation phase, the phase current is zero and so is the back emf and it begins to build up as the phase currents goes up. The emf direction supports phase build up when a positive voltage is applied to the phase winding. When source voltage is turned off, the phase current build up is supported entirely by the emf. Power generation begins during the demagnetization when the generator phase winding is subjected to a negative source voltage or connected to a load. The phase current magnitude during this period depends on the magnitude of the emf and the supply voltage. A typical inductance and current waveforms of a SRG are shown in Fig. 2.

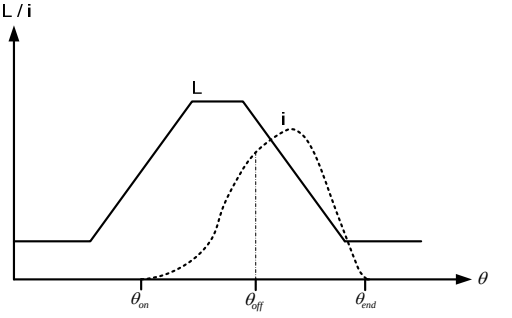

Fig. 2. The typical inductance and current waveforms of a SRG

A stator phase winding is energized during the rising part of the inductance profile hence, the turn-on angle falls before the fully aligned rotor/stator poles positions and the turn off angle falls during the negative slope of the inductance profile which is located after the fully aligned position, during this period the machine generates power back into the supply or the load. The excitation period begins from θ_{on} to θ_{off} and that is when an external voltage supply is applied to the stator phase winding. The period from θ_{off} to θ_{end} in which the energy stored in the stator winding is released through diodes or two-switch per phase winding till the phase current reaches zero is called the generation mode.

3. OPERATING THEORY OF SRG

Although saturation plays an important role in obtaining the exact behavior of the SRG, and also is necessary for the detailed generator design but the analysis of the magnetically linear SRG can provide the useful and broad understanding of the influence of the many generator parameters.

The equation for the SRG phase voltage shown in Fig. 1 can be expressed as follows:

$$V = Ri + \frac{\partial \lambda(\theta,i)}{\partial t} \quad (1)$$

Where istands for the generator phase current and λ for the flux linkage which is a function of both the phase current and rotor position therefore, equation (1) can be rewritten as:

$$V = Ri + \frac{\partial \lambda}{\partial i}\frac{\partial i}{\partial t} + \frac{\partial \lambda}{\partial \theta}\frac{d\theta}{dt} \quad (1)$$

For a given current, L is a function of rotor position and a linear quantity. Hence equation (2) can be rewritten as:

$$V = Ri + L(\theta)\frac{di}{dt} + i\omega\frac{dL(\theta)}{d\theta} \quad (2)$$

The last part of (3) is the back emf. The analysis of the back emf gives an important insight into the SRG operation. First, the back emf is a function of the phase current, machine speed and phase inductance. Second, the back emf polarity depends on the inductance variation. During the generation mode, which occurs in the period of the decreasing phase inductance, the back emf is negative.

4. FORMULATION AND ANALYSIS OF THE GENERATOR/MOTOR

The solution to the equation (3) yields the following result for the current i:

$$i = \frac{V_s}{R + \frac{dL}{d\theta}\omega} + [I_0 - \frac{V_s}{R + \frac{dL}{d\theta}\omega}]e^{-\frac{t}{\tau}} \quad (3)$$

Where, I_0 stands for the initial current, and

$$\tau = \frac{L(\theta)}{R + \frac{dL(\theta)}{d\theta}\omega} \quad (4)$$

In order to be able to plot the current profile for a SRG, the parameters in (2) are found by either numerically or experimentally for a 6 by 4, three phase, 30 V switched reluctance generator with the following specifications:

Stator core outer diameter	= 72 mm
Stator core inner diameter	= 62 mm
Rotor pole arc	=32°
Stator pole arc	=28°
Stack length	=35 mm
Air gap	= 0.25 mm
Rotor core outer diameter	= 39.5 mm
Rotor shaft diameter	= 10 mm
Number of turns per pole	= 75

In the numerical part, the magnetic field analysis has been performed using a commercial finite element package [15], which is based on the variation energy minimization technique to solve the magnetic vector potential.

For the finite element analysis a second order triangular element with dense meshes at places where the variation of fields are greater has been used. In the present study, it has been assumed that each phase of the motor is excited by the rectangular blocks of the current. Also, the usual assumptions have been considered for analyzing such as: the magnetic field outside the motor periphery is zero, the magnetization curve is single valued, the end effects are neglected and the magnetic vector potential and current density vector have only z-directed components. For convenience the position of a stator pole when is in the opposite of a rotor pole such that the reluctance of the motor magnetic structure is minimum, is defined as the aligned position. The unaligned position is defined as that when the rotor pole is in the opposite of the stator slot such that the reluctance of the motor magnetic structure is at its maximum. In the analysis the rotor moves from unaligned to aligned position hence, all the motor parameters for these points in between can be computed. This simulation directly yields prediction of the flux linkages. The contour plots of the flux inside of each motor lamination for two different rotor positions are shown in Figs. 3a and 3b.

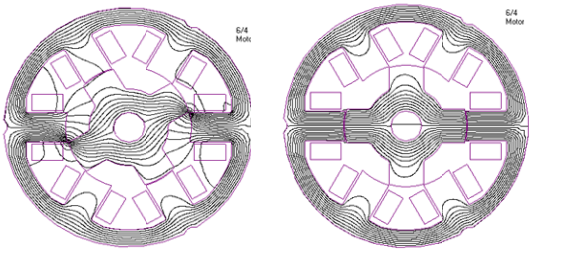

a) The unaligned case b) The aligned case

Fig. 3. The Contour plots of the flux line inside the motor lamination

The so called "effective" inductance has been defined as the ratio of each phase flux linkage to the exciting current (λ / I). The values based on this definition are presented in fig. 4 for the under investigation generator. In the analysis the rotor moves from fully unaligned (i.e.-45°) to completely aligned (i.e. 0°) and then to fully unaligned (i.e. +45°) positions.

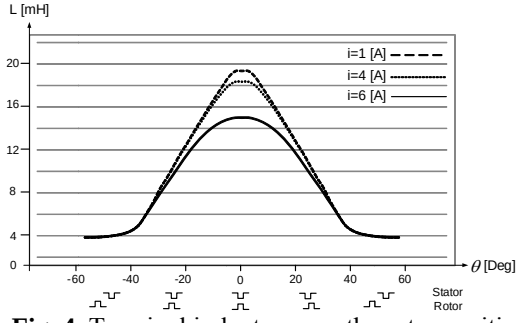

Fig. 4. Terminal inductance vs the rotor position

In the unaligned position the "effective" inductance is at its lowest value and increases as the generator goes into the aligned position. This inductance increase is due to the fact that the reluctance of the generator magnetic circuit decreases as the rotor moves into the aligned position. The minimum and maximum values of inductance for the different current values are shown in fig.4. In this analysis the maximum and minimum effective inductance values used in the calculations are 4mH and 18mH, respectively.

Substituting these inductance values into (4), and for a speed of 5000 rpm the current for the different regions of the inductance profile has been evaluated. In every region the value of the inductance considered to be constant for a very short period of time in order to be able to compute the value of the current in (4). Fig. 5 shows the current waveform for the entire inductance profile shown in Fig. 3. It is worth mentioning that the current computed and plotted from the time when the switch S1 is closed which is at 15^0 before the start of the rotor/stator poles alignment till the switch is turned off at 9^0 in the negative slope of the phase inductance. During the generation mode the current discharges into a18Ω resistive load.

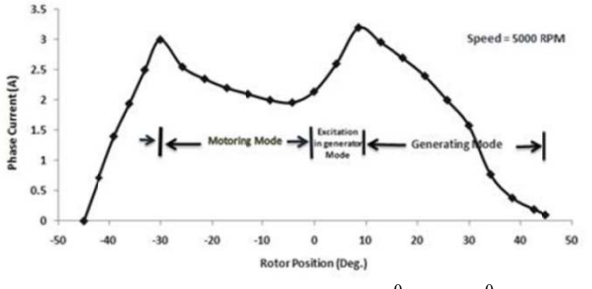

Fig. 5. Current waveform from -45^0 to $+45^0$ of the rotor position

The different parts of the current waveforms in Fig. 5 may be explained with reference to the simulated inductance profile of Fig. 3. The phase winding is connected via switch S_1 to the voltage source Vs at t=0 or $\theta=-45^0$ while the phase inductance is at its lowest value and is roughly constant, thus permitting current builds up at almost a fast rate until the phase inductance begins to increase $\theta= -30^0$. The positive rate of the change of the phase inductance with time causes the current to fall. The current now is flowing through the switch S_1 and also decaying due to the higher inductance value. At zero degree position the value of the current has reached to about 2 A. A little bit after this time the rate of the inductance with respect to the θ is negative and switch S1 is still on, hence the current builds up now is due to the negative sign of the back emf. During this period the current flows from the supply and energy is stored in the machine. This energizing period is known as the excitation time and is necessary because the SR machine is a singly excited machine. At 9^0 rotor position S1 is turned off and all of the stored energy will be released to the resistive load during the negative slope of the inductance profile, hence the current falls off during this period which is known as the generating mode. Fig. 6 shows the current waveforms at two different speeds but the same start points with the on/off periods of the switch S_1.

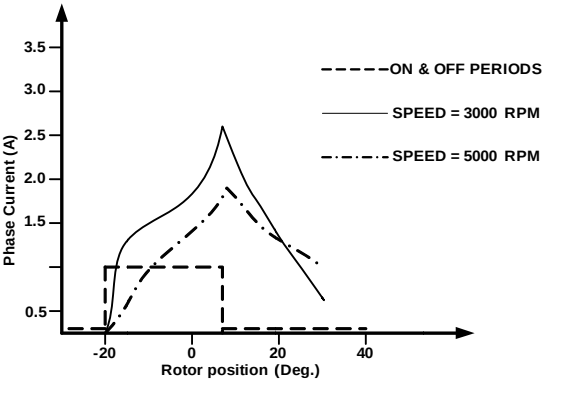

Fig. 6. Current waveforms for the two different speeds

As inferred from the current waveforms, when the motor speed is higher the stator phase current is smaller in the exciting as well as generating modes. More advancement in the conduction angle produces the larger current at high speeds before exciting mode; hence the higher back emf is achievable and the more generating power can be produced.

Fig. 7 shows the effect of advancing on the phase current at 5000 RPM, for three different advancement angles using (4) in the SRG.

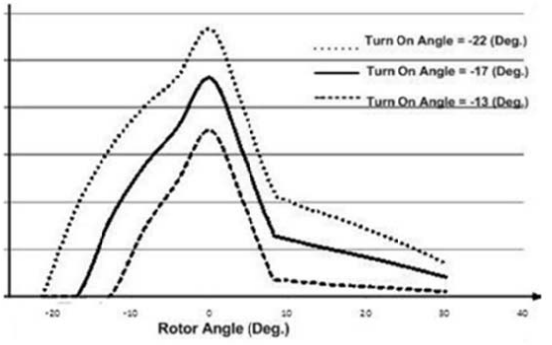

Fig. 7. The phase current at 5000 RPM, for three different turn on advancement angles

In order to see the shape of the actual current waveforms under the different turn on angles, a set of optical sensors, having adjustable positions with respect to the rotor poles are fixed at the end of the 6 by 4 switched reluctance generators. Figs. 8.a, 8.b, and 8.c show the actual generator phase current waveforms in the main windings as well as the on time period of the power switches at the different speeds versus the time having 15^0 advancement angle, respectively.

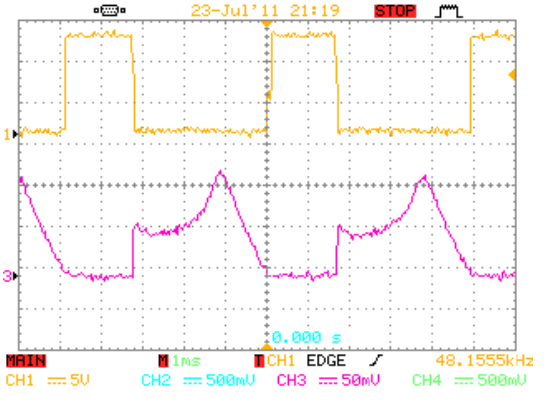

(a) 3000RPM and 15^0adv.

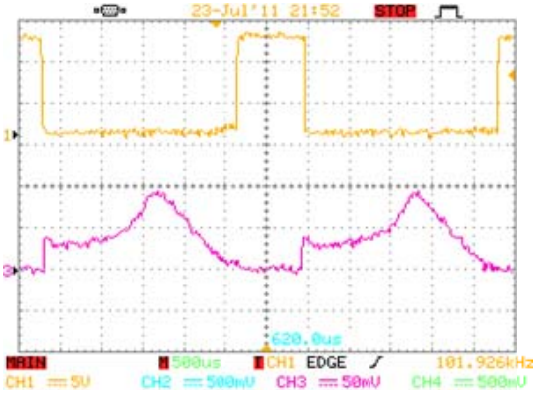

(b) 5000 RPM and 15^0 adv

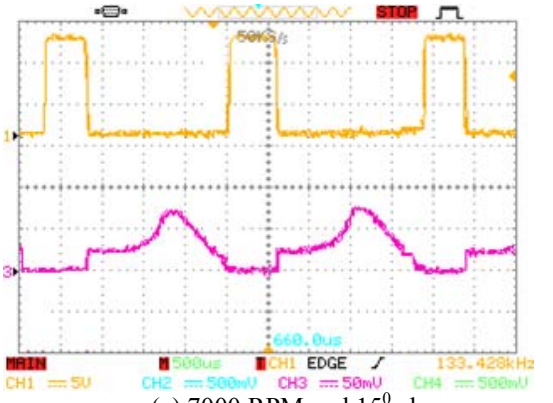

(c) 7000 RPM and 15^0adv

Fig. 8. The generator on time period of the two power switch phase currents in the main winding

As seen in Figs. 8(a), 8(b), and 8(c) the shape of the current changes as the speed of the generator prime mover goes up. Having different current slopes during the discharge is due to the different time constants for the duration of the negative rate of the inductance with respect to the rotor position and also time constant after the rotor pole leaves the stator pole. The oscilloscope probe is set to ×10 to measure the output current waveform. One phase generator current at different speeds for an applied constant field voltage of 12V but the same advancement angle for the transistor firing time is shown in Fig. 9.

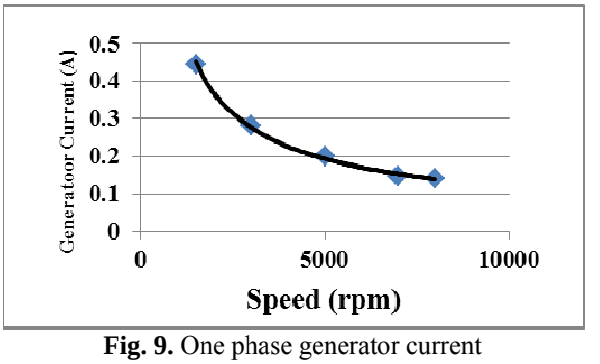

Fig. 9. One phase generator current

As seen in Fig. 9 the current drops exponentially as the speed goes up. The main reason is due to $R+\frac{dL}{d\theta}\omega$ in the denominator of the equation (4).

The motoring mode of the operation saturation plays an important role in obtaining the exact behavior of the SRM drive and also, is necessary for the detailed motor design, but the analysis of the linear SRM drive magnetically can provide useful and broad understanding of the influence of the many motor parameters.

Fig. 10 shows the variation of the inductances with respect to the rotor position for only one pair of the stator poles in an ideal linear motor shown in Fig. 1.

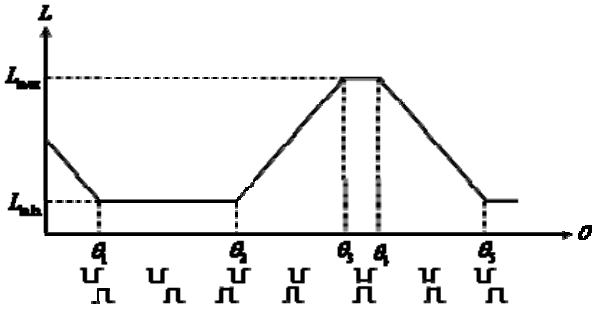

Fig. 10. Inductance variation of one motor phase

The positions of the rotor pole with respect to the stator pole corresponding to the different parts of the inductance profile are also shown in Fig. 10 Substituting these inductance values into equation (4) and for a speed of 5000 rpm, the currents of the different regions of the inductance profile have been evaluated. The current was computed for the time when the switches S1 and S2 are open, during this time the polarity of the power supply is reversed and current flows through diodes D_1 and D_2. Fig. 11(a) and (b) show the current waveforms for different advancements in the conduction angle. It is worth mentioning that all the current curves have been plotted starting at t = 0 to be compared.

(a) 5 Deg. Advancement

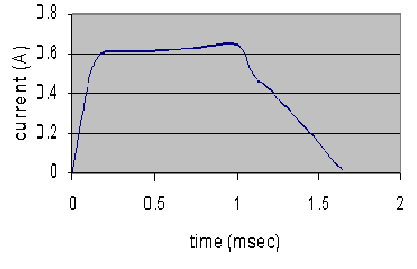

(b) 14 Deg. Advancement

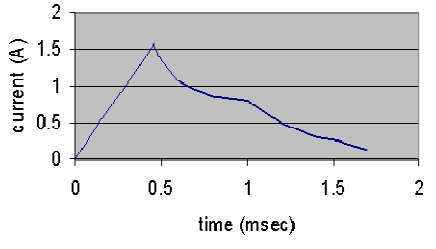

Fig. 11. a) Current waveform for 5 Deg. of Advancement
b) Current waveform for 14 Deg. of Advancement

The different parts of the current waveforms of Figs. 11(a) and 11(b) may be explained with reference to the positions of the idealized inductance profile of Fig. 10 using the circuit shown in Fig. 1. The phase winding is connected via switches S_1 and S_2 to the voltage source Vs at t = 0 while the phase inductance is low (i.e. $\theta_1 \langle \theta \langle \theta_2$), thus permitting current build up at almost linear rate until the phase inductance begins to increase (i.e. $\theta_2 \langle \theta \langle \theta_3$). The positive rate of the change of the phase inductance with the time causes the current to fall. From then on the switches are open and the voltage source is connected to the phase winding via the diodes D_1 and D_2. The current now is flowing through the diodes and also decaying fast. As seen from the current waveforms, the more advancement in the conduction angle produces the larger current in the high speed hence, the higher torque is obtainable. The phase advancing can also cause the phase commutation to end before the rotor reaches the negative torque region (i.e. $\theta_4 \langle \theta \langle \theta_5$).

Timing at 5 msec/div. , Current at 2 A/div.

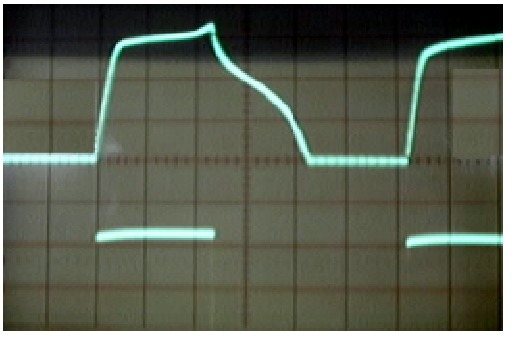

Fig. 12. a) Actual current waveforms for 5 Deg. of the advancement
b) Power switches turn on time duration

Timing at 5 msec/div., Current at 5 A/div.

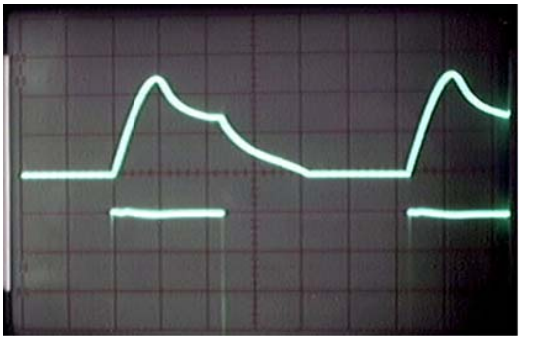

Fig. 13. a) Actual current waveforms for 14 Deg. of the advancement
b) Power switches turn on the time duration

In order to see the shape of the actual current waveforms under the different turn on angles, a set of optical sensors, having adjustable positions with respect to the rotor pole is fixed at the end of the 6×4 switched reluctance motor. Figs 12(a),(b) and 13(a),(b) show the actual motor phase current waveforms and the on time duration of the power switches under 5 and 14 degrees of advancing for the phase turn on angles at a speed of 5000 rpm, respectively.
Comparisons between the actual current waveforms in figs. 12(a) and 13(a) and the computed ones in Figs. 11a and 11b show the close agreement in general shape of the waveforms and a difference of less than 14% of the magnitudes. The reason for the difference is due to the assumptions made in writing and solving the equation (1).

5. EXPERIMENTAL STUDY

Advanced conduction angle at the generator starting phase (i.e. i_{phase}=0) can have profound effect on the power production mechanism since the higher current is achievable before and during the exciting mode. At the medium and high speeds, but low advanced turn on angle, the current does not build up enough before the exciting mode to produce the required output voltage due to the generator back emf effect. The amount of the advance at the different speeds to produce the needed output voltage cannot be a fixed value. Therefore, a means of producing variable advancements in the commutation angle for the different speeds is required.
There are three 30° pulses produced by the generator shaft position sensors in every 90° of shaft rotation. These pulses are fed into a pulse-shaping unit in order to get 3 pulses series of 30° width per 90° revolution as shown in Fig. 14(a), and 14(b).

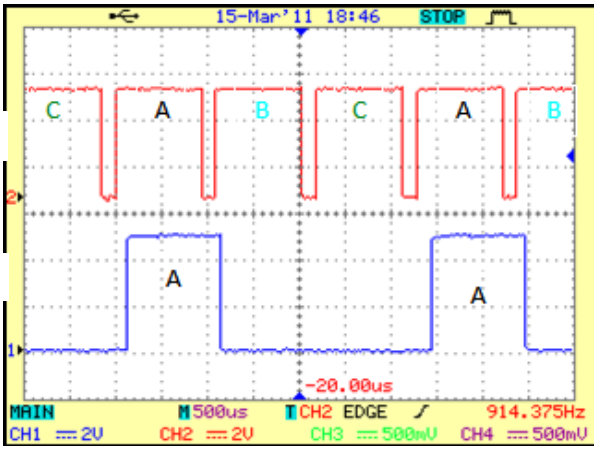

(a)

(b)

Fig. 14. a) The output of the pulse shaping unit
b) The generator pulses of phase A

The frequency of this pulse train is increased to 30 times higher by employing a P.L.L. module. The P.L.L. module comprises of a CMOS 4046 and a 40102 counter integrated circuits. The P.L.L. output produces a pulse train with one-degree resolution in comparison with the original 30° generator pulses. In the other word, there are thirty pulses embedded in every 30° of the generator position sensor as shown in Fig. 15.

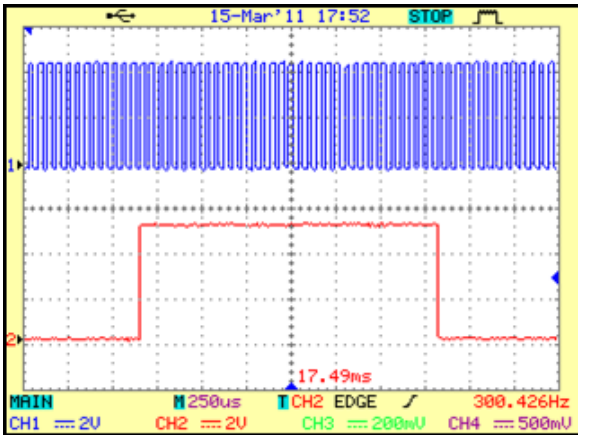

(a)

(b)

Fig.15a) The generator pulses of the phase A.
b) The output of the P.L.L. module**.**

Fig. 15(a) shows the output of the P.L.L. module which covers the all three signals from the position sensors, while fig. 12(b) depicts only the phase A sensor output pulse. This pulse train and the pulse shaping unit output signal are fed into the counter module. The amount of the phase turn on the advancement variation is set by an 8051 Intel microcontroller, which measures the generator output voltage. A predefined look-up table for the output voltage/advancement angle will generate the proper advancement angle. This table is used in this paper because the assumption of the high speed was made at the beginning. It is possible to expand this table to include the generator speed, the output voltage and the amount of the advancement angle as well. In this way, if the generator is running at slow speeds only the pulse width modulation for the field current should act and set the output voltage. If the generator speed goes higher than some preset values such that it would not be able to produce the desired output power then PWM is kept constant at 100% and advancing of the turn on angle begins. The user can define this table in any desired way. The program flowchart for the microcontroller is shown in Fig. 16.

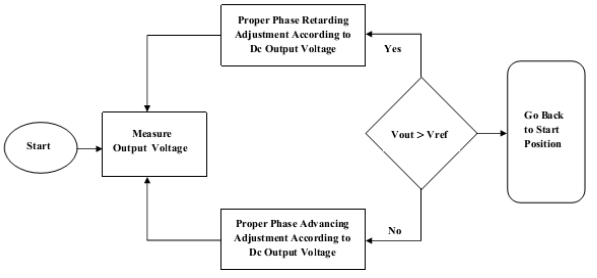

Fig.16 Theprogram flowchart of the microcontroller

The counter module output pulses are separated into three independent advanced generator pulse trains by a demultiplexer. Figs 17(a), 17(b), 18(a), 18(b) and 19(a), and 19(b) show the original pulse trains from the generator shaft sensors after 0^o , 5^o and 15^o degrees firing angle adjustments for phase A, respectively. It is worth mentioning that the original pulses from the generator position sensors are set at 15^o advance (i.e. θ=-30^0.)as the base of the microcontroller calculations. A As the generator speed increases, a time delay will be produced by the microcontroller with respect to the position sensors output pulses. In the other words, the produced pulses are advanced with reference to the start of the machine's exciting and generating periods.

(a)

(b)

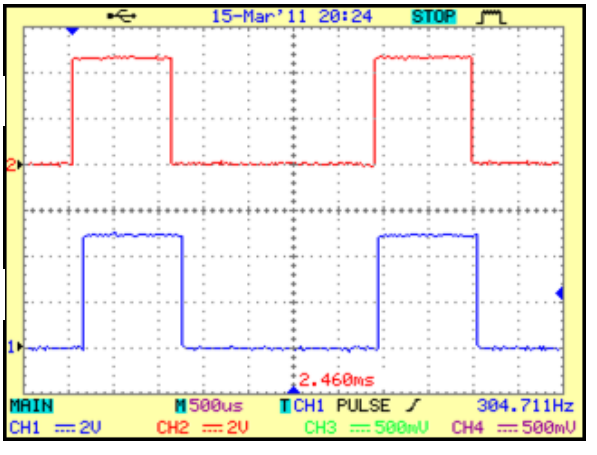

Fig. 17. a) The original generator pulses
b) The pulses after 0^o advancing

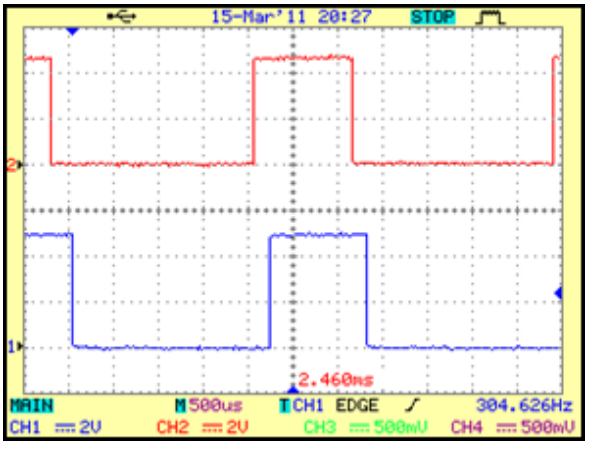

Fig. 18. a) The original generator pulses
b) The pulses after 5^o advancing

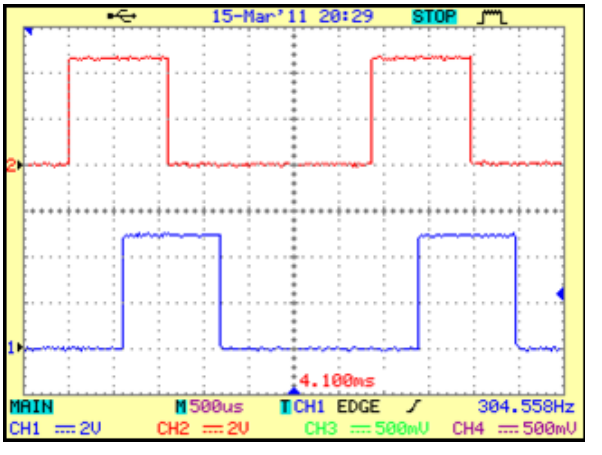

Fig.19. a) The original generator pulses
b) The pulses after 15^o advancing

As shown in Figs. 17 through 19 the pulses going into the generator drive circuit are delayed compared to the position sensors pulses which in turn are translate to producing pulses which are advanced in the reference frame of the machine's generating mode.

In order to see the effect of the change in turn onangle experimentally for the motoring mode, the following two tests have been performed.

Test 1:Setting the turn on angle first at 5 and then at 14 degrees fixed in advance meaning, the electronic governor is locked so there will be any changes in these angles, then the torque, speed, and current are measured and plotted. Figs. 20 and 21 show the plots of the speed versus the torque and the torque versus the current, respectively.

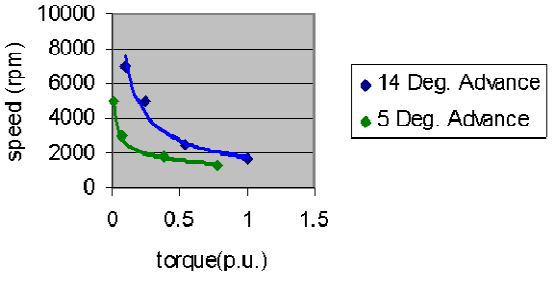

Fig. 20. Speed vs. torque

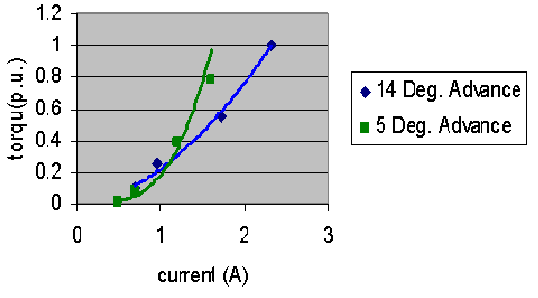

Fig. 21. The torque vs the current

As seen in Fig. 20, the higher speed -torque curve has been obtained for the14 Deg. advancement while Fig. 21 shows that the larger torque has been achieved only for the current less than 1.1 A, but the higher output power.

Test 2: The governor is used for the automatic advancement of the firing time with three different settings for the governor such that, the advancement of the turn on angles are adjusted for 0-6, 0-10, and 0-14 degrees, respectively under the same loading condition. Fig. 22 shows the speed-torque characteristics of the motor under the same loading condition for the different settings of the governor.

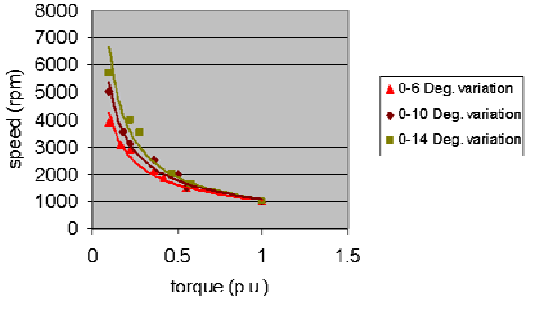

Fig. 22. Thespeed torque characteristics of the motor under different governor settings

As shown in Fig.15, the curves have converged to a point at full load since the governor has reached its final setting completely at 1000 rpm. At light loads in the high speed, the curves have been separated apart since the advancing angle for each one is different. The curve for the 0-14 degrees variation shows the highest torque value for the same speed.

Fig. 23 shows the torque-current characteristics of the motor with the same conditions mentioned for the Fig. 22.

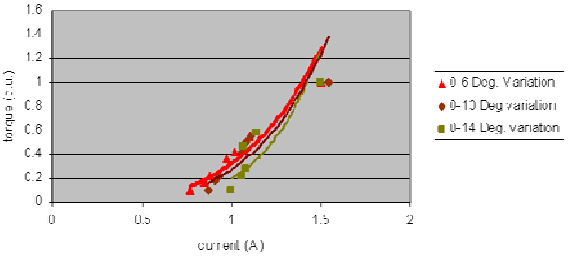

Fig. 23. The torque current characteristics of the motor under the different governor settings

The motor current under 0-14 angle variation has the highest value for the same torque and all curves reach to the same point at full load. It is worth mentioning that the curve fitting has been used in plotting the data in Figs. 22 and 23. The reason for the lower torque production in the large variation angle is due to having smaller on time current period in the torque producing region.

6. CONCLUSION

An electronic circuit has been built and employed for a 6 by 4 SRG as well as SRM. This circuit causes the phase commutation to begin sooner and end sooner, therefore the current has sufficient time to build up to the proper level before it reaches the generator excitation mode. The amount of the phase commutation advancing which is related to the generator output voltage is obtained from a desired voltage/angle table programmed into the microcontroller. The test results using this circuit show a great improvement and control in keeping the output voltage at the desired level at variable high speeds. This technique solves one of the drawbacks of the switched reluctance generators especially at high variable speed. The general shapes of the current waveforms found experimentally support and the results obtained numerically. The difference between the current values found by these two methods is within 15% and this variation is due to the assumptions made in the magnetic circuit of the generator for developing the current equation.

REFERENCES

[1] D. Susitra, E. Annie, and E. Jebaseeli, **"Switched Reluctance Generator-Modeling, Design, Simulation, Analysis and Control A Comprehensive Review",** *International Journal of Computer Applications*, Vol. 1, No. 2, 2010, pp. 10-16.

[2] A. Takahashi, H. Goto, K. Nakamura, T. Watanabe, and O. Ichinokura, **"Characteristics of 8/6 Switched Reluctance Generator Excited by Suppression Resistor Converter"**, *IEEE Transactions on Magnetics*, Vol. 42, No. 10, Oct., 2006.

[3] A. David Torrey, **"Switched Reluctance Generators and Their Control"**, *IEEE Transactions on Industrial Electronics*, Vol. 49, No. 1, Feb. 2002, pp. 556-565.

[4] A. Takahashi, H. Goto, K. Nakamura, T. Watanabe, and O. Ichinokura, **"Characteristics of 8/6 SR Generator with a Suppression Resistor Converter"**, *IEEE International Conference On Power Electronics and Motion Control*, EPE-PEMC 2006, Portoroz Slovenia, pp. 1037-1041, Sep. 2006.

[5] N. Radimov; N. Ben-Hai; R. Rabinovici, **"Switched Reluctance Machines as Three-Phase AC Autonomous Generator"**, *IEEE Transactions on Magnetics*, Vol. 42, Issue 11, pp. 3760 -3764, October 2006.

[6] D. McSwiggan, L. Xu, and T. Littler, **"Modelling and Control Of A Vriable-Speed Switched Reluctance Generator Based Wind Turbine"**, UPEC 2007, pp. 459-463.

[7] L. Hoang; M. Chakir, **"Optimizing The Performance of a Switched Reluctance Generator By Simulation"**, *IEEE International Conference on Electrical Machines*, ICEM 2010, Suntec Singapore, September 2010.

[8] R. C´ardenas, R. Pe˜na, M. Pe´rez, J. Clare, G. Asher and P. Wheeler, **"Control of a Switched Reluctance Generator for Variable-Speed Wind Energy Applications"**, *IEEE Transactionson Energy Conversion*, Vol. 20, No. 4, pp. 781-791, December 2005.

[9] B. Fahimi, A. R. B. Emadi, and Jr. Sepe, **"A switched reluctance machine based starter/alternator for more electric cars"**, Energy Conversion, *IEEE Transactions on* , Vol. 19 , No. 1, pp. 116-124, March 2004.

[10] E. Richter, C. Ferreira, "**Performance evaluation of a 250 kW switched reluctance starter generator,"** *Conf. Rec. 1995 IEEE IndustryApp*., Vol. 1, pp. 434–440, 1995.

[11] P. Asadi, M. Ehsani, and B. Fahimi, **"Design and Control Characterization of Switched Reluctance Generator for Maximum Output Power"**, *IEEE Annual Conference on Applied Power Electronics*, 2006, APEC '06, Texas, March 2006.

[12] S. Dixon, B. Fahimi, **"Enhancement of output electric power in switched reluctance generators"**, Electric Machines and Drives Conference, 2003, *IEMDC'03. IEEE International 1-4,* Vol. 2. pp. 849-856, June 2003.

[13] D. A. Torrey, **"Switched reluctance generators and their control,"** *IEEE Trans. Ind. Electron*, Vol. 49, No. 1, pp. 3-14, Feb. 2002.

[14] E. Afjei and M. R. Sahebi, **"Automatic Phase Advancing in Switched reluctance Motor by Employing An Electronic Governor For A Desired Speed Angle Profile"**, *International Journal of Engineering*, Vol. 17, Transactions A: Basics, pp. 11-18, February 2004.

[15] Magnet CAD Package: User Manual, Infolytica Corporation Ltd., Montreal, Canada, 2006.